Elaboration of Densely Functionalized Polylactide Nanoparticles from *N*-Acryloxysuccinimide-Based Block Copolymers

NADÈGE HANDKÉ,[1] THOMAS TRIMAILLE,[1] ELSA LUCIANI,[2] MARION ROLLET,[1] THIERRY DELAIR,[3] BERNARD VERRIER,[2] DENIS BERTIN,[1] DIDIER GIGMES[1]

[1]Laboratoire Chimie Provence (LCP), UMR 6264, Universités d'Aix-Marseille I, II et III - CNRS, Equipe Chimie Radicalaire Organique et Polymères de Spécialité, Case 542, Av. Escadrille Normandie-Niemen, 13397 Marseille Cedex 20, France

[2]Institut de Biologie et de Chimie des Protéines (FRE 3310), Université Lyon 1 - CNRS, 7 Passage du Vercors, 69367 Lyon, France

[3]Laboratoire des Matériaux Polymères et Biomatériaux (UMR 5223), Université Lyon 1 - CNRS, 15 Boulevard Latarjet, 69622 Villeurbanne, France

Received 12 November 2010; accepted 20 December 2010
DOI: 10.1002/pola.24553
Published online 18 January 2011 in Wiley Online Library (wileyonlinelibrary.com).

ABSTRACT: Poly(*N*-acryloxysuccinimide) (PNAS) and poly(*N*-acryloxysuccinimide-*co*-*N*-vinylpyrrolidone) (P(NAS-*co*-NVP)) of adjustable molecular weights and narrow polydispersities were prepared by nitroxide-mediated polymerization (NMP) in *N*,*N*-dimethylformamide in the presence of free SG1 (*N*-*tert*-butyl-*N*-1-diethylphosphono-(2,2-dimethylpropyl) nitroxide), with MAMA-SG1 (*N*-(2-methylpropyl)-*N*-(1-diethylphosphono-2,2-dimethylpropyl)-*O*-(2-carboxylprop-2-yl)hydroxylamine) alkoxyamine as initiator. The reactivity ratios of NAS and NVP were determined to be $r_{NAS} = 0.12$ and $r_{NVP} = 0$, indicating a strong alternating tendency for the P(NAS-*co*-NVP) copolymer. NAS/NVP copolymerization was then performed from a SG1-functionalized poly(D,L-lactide) (PLA-SG1) macro-alkoxyamine as initiator, leading to the corresponding PLA-*b*-P(NAS-*co*-NVP) block copolymer, with similar NAS and NVP reactivity ratios as mentioned above. The copolymer was used as a surface modifier for the PLA diafiltration and nanoprecipitation processes to achieve nanoparticles in the range of 450 and 150 nm, respectively. The presence of the functional/hydrophilic P(NAS-*co*-NVP) block, and particularly the *N*-succinimidyl (NS) ester moieties at the particle surface, was evidenced by ethanolamine derivatization and zeta potential measurements. © 2011 Wiley Periodicals, Inc. J Polym Sci Part A: Polym Chem 49: 1341–1350, 2011

KEYWORDS: block copolymers; functionalized poly(D,L-lactide) nanoparticles; nitroxide-mediated polymerization; *N*-acryloxysuccinimide; *N*-vinylpyrrolidone

INTRODUCTION Because of their properties of biocompatibility and biodegradability, polylactide (PLA)-based nanoparticles (NP) have a long history in the field of drug delivery[1,2] and are still attractive candidates.[3] The now classically used PLA-based NP carriers are surface coated with hydrophilic "stealth" polymers such as poly(ethylene oxide) (PEO) that are efficient for reducing NP uptake by the reticular endothelial system (RES) and thus prolonging their circulation in the blood stream.[4] By far, this was mainly achieved by the use of PEO-*b*-PLA or PEO-*b*-poly(propylene oxide) (PPO)-*b*-PEO (Pluronics) amphiphilic block copolymers as surface modifiers during the fabrication process of the nanoparticles. One major remaining challenge for drug carrier engineering is the possibility to further couple cell specific ligands on this hydrophilic corona to envision "active" targeting drug delivery. However, PEO, as a polyether, can hardly be functionalized along its backbone for further ligand coupling and up to now, the most used approach has been to exploit the PEO end group of the PLA-PEO block copolymer to introduce the ligand moieties through various functionalization chemistries.[5,6,7,8] As a result, the surface density of ligands at the micelle or particle surface is somehow limited (one ligand per chain). In this context, we aimed at developing block copolymers containing a PLA block and a block bringing both hydrophilicity and functional group along the backbone for biomolecule coupling, namely a poly(*N*-vinylpyrrolidone-*co*-*N*-acryloxysuccinimide) (P(NVP-*co*-NAS)) block. The NAS units present reactive *N*-succinimidyl (NS)-activated esters that can indeed efficiently react with the amino-bearing molecules,[9] whereas NVP ones have to confer hydrophilic/stealthy properties. NVP is gaining increasing attention, because of the biocompatibility and low toxicity of its corresponding polymer, which makes it a viable alternative to poly(ethylene gycol) regarding stealth properties.[10]

Our envisioned PLA-based block copolymer requires to combine both ring-opening polymerization (ROP) and controlled radical polymerization (CRP) techniques. It is to point out

Additional Supporting Information may be found in the online version of this article. Correspondence to: T. Trimaille (E-mail: thomas.trimaille@univ-provence.fr)

that such combination has strongly emerged over the last years to achieve well-defined block copolymers made of aliphatic polyester and vinyl polymer segments, as reviewed by Dove,[11] either through ROP/atom transfer radical polymerization (ATRP),[12] ROP/reversible addition fragmentation chain transfer (RAFT),[13] or ROP/nitroxide-mediated polymerization (NMP)[14] combined techniques. We particularly reported in a previous article the convenient access to PLA-*b*-poly(hydroxyethyl (meth)acrylate) and PLA-*b*-polystyrene block copolymers through the ROP/NMP combination.[15] Our strategy is based on the use of a SG1 nitroxide functionalized PLA as macro-alkoxyamine to initiate NMP of the vinyl monomer(s) of interest. Regarding the NAS/NVP vinyl monomer system envisioned here for the "radical" made block, CRP techniques have not been reported to our knowledge. Indeed, whereas copolymerization of NAS with other comonomers has been extensively reported via the CRP techniques, principally by RAFT (*N*-isopropylacrylamide (NIPAM),[16] NIPAM and fluorescein *O*-methacrylate,[17] *N,N*-dimethylacrylamide (DMA),[18,19,20] hydroxyethylacrylate (HEA),[21] or *N*-acryloylmorpholine (NAM)[22,23,24]) and to a less extent by ATRP (styrene[25]) and NMP (DMA),[26] its copolymerization with NVP has only been reported by conventional radical polymerization.[27] We here successively describe the synthesis by NMP of P(NAS-*co*-NVP), PLA-*b*-P(NAS-*co*-NVP) block copolymers and their use as surface modifier in PLA nanoprecipitation and diafiltration processes to achieve novel PLA nanoparticles with advanced functional/hydrophilic surface properties.

EXPERIMENTAL

Materials

N-Hydroxysuccinimide (NHS, 98%), acryloyl chloride (96%), triethylamine (TEA, 99%), *N*-vinylpyrrolidone (NVP, 99%), and 1,3,5-trioxane (99%) were purchased from Aldrich. The MAMA-SG1 alkoxyamine (BlocBuilder MA, 99%) and the SG1 nitroxide (82%) were kindly provided by Arkema. Poly(D,L-lactide) (PLA50 M_n = 30,000 g/mol, PDI = 1.7) with a carboxylic end group was purchased from Phusis (Grenoble, France). PLA-SG1 macro-alkoxyamine was synthesized as previously described.[15] All NMR solvents were purchased from Eurisotop. All the solvents were used as received.

N-Acryloxysuccinimide Synthesis

N-acryloxysuccinimide (NAS) was synthesized according to a previously reported procedure.[28] In brief, it consists in direct reaction of NHS and acryloyl chloride in presence of TEA. A solution of acryloyl chloride (18 mL, 0.22 mol) in chloroform (30 mL) was added dropwise to a stirred solution of NHS (22.65 g, 0.196 mol) and TEA (30 mL, 0.22 mol) in chloroform (300 mL) at 0 °C. After stirring 3 h at 0 °C, the reaction mixture was washed with ice-cold saturated sodium bicarbonate solution three times and dried over $MgSO_4$. Then, the solution was filtered and chloroform was removed under reduced pressure until a residual volume of 60 mL. The product was precipitated overnight at −18 °C after the dropwise addition of a mixture of hexane and ethyl acetate (80:12 mL). The product was filtered and washed successively with 200 mL of hexane:ethyl acetate mixture (4:1), then (9:1) and with 400 mL of pure hexane. The final product was dried under vacuum to a constant weight (24.6 g, 74% yield).

^{1}H NMR (300 MHz, $CDCl_3$, δ, ppm): 2.87 (s, 4H), 6.16–6.20 (dd, 1H), 6.29–6.38 (dd, 1H) 6.68–6.74 ppm (dd, 1H). Anal. Calcd for $C_7H_7NO_4$: C, 49.71; H, 4.17; N, 8.28. Found: C, 49.79; H, 4.23; N, 8.30.

Polymer Synthesis

The homopolymerization of NAS from the MAMA-SG1 alkoxyamine was carried out in DMF (25 wt % monomer content) in the presence of free SG1 (0, 2.5, 5, or 7.5 mol % to initiator). 1,3,5-Trioxane was used as internal ^{1}H NMR reference in the mixture to follow the conversion of the monomer. Typically, NAS (1 g, 5.92 mmol) and MAMA-SG1 alkoxyamine (38.5 mg, 0.1 mmol, for a targeted M_n of 10,000 g mol^{-1}) were introduced in a 25-mL two-neck round-bottomed flask fitted with a reflux condenser and an argon inlet and deoxygenated for 20 min by argon bubbling. The mixture was then heated to 110 °C under argon with vigorous stirring. After polymerization, the mixture was cooled down and precipitated in diethyl ether. During the polymerization, samples were withdrawn periodically for determining conversion and molecular weight by ^{1}H NMR and GPC, respectively. The final polymer was purified by precipitation in diethyl ether and dried under vacuum at room temperature to a constant weight.

Copolymerization of NAS and NVP was performed under a similar procedure from the MAMA-SG1 alkoxyamine, with an overall monomer concentration of 1 mol L^{-1} in DMF. The mixture was heated to 100 °C. Different M_n values (10,000, 20,000, and 40,000 g mol^{-1}) were targeted using 5 mol % of free SG1 to initiator. The final polymer was purified by precipitation in diethyl ether and dried under vacuum at room temperature to a constant weight. NAS/NVP copolymerization from the PLA-SG1 macro-alkoxyamine was performed under a similar procedure, except that polymerization temperature was 120 °C and precipitation was performed in diethyl ether/methanol (1/1) mixture.

Characterization

^{1}H NMR (300 MHz) spectra were recorded on a Bruker Avance DPX-300 at room temperature. For organic compounds analysis were performed with 10 mg in 500 μL of $CDCl_3$. The polymerization kinetics was studied with 60 μL of mixture in 500 μL of DMSO-d_6. For determination of NAS and NVP conversions, the peak integrals of the vinyl protons (6.3–6.8 ppm and 6.9–7.05 ppm for NAS and NVP, respectively) and 1,3,5-trioxane (5.13 ppm) were used. Elemental analyses on NAS were performed on a Thermo Finnigan EA 1112 (Spectropole, Marseille).

The number-average molar molecular weight (M_n) and the polydispersity index (PDI) were determined using gel permeation chromatography (GPC). The homo- or co-polymer samples were prepared using 5 mg of the polymer in 2 mL of

DMF and then filtered on nylon Millipore Millex GN syringe filter. The GPC chain consisted of a Waters 717 plus autosampler, a Waters 600 system controller and a Waters 600 fluid unit. A waters 2414 differential refractometer was used at 40 °C as detector. DMF was used as eluent at a flow rate of 0.7 mL min^{-1} after filtration on Alltech nylon membranes with a porosity of 0.2 μm. The column oven was kept at 70 °C, and the injection volume was 20 μL. Two ResiPore columns (600 mm × 7.5 mm), Polymer Laboratories, were used in series. The system was calibrated using polystyrene (PS), poly(methyl methacrylate) (PMMA) or polyethylene glycol (PEG) narrow standards, in the range 1000–400,000, purchased from Polymer Laboratories.

Reactivity Ratios

Several copolymerizations of NAS and NVP were carried out by NMP targeting constant total degree of polymerization (300). Different initial feed in NAS and NVP monomers were used: 0.2/0.8, 0.3/0.7, 0.5/0.5, 0.7/0.3, and 0.8/0.2. The reactivity ratios r_1 and r_2 were determined using a nonlinear least square method, as previously reported,[29,30,31] based on fitting experimental values of conversion and theoretical ones obtained from the integrated copolymerization eq 1 developed by Lowry and Meyer.[32]

$$1-\frac{[M]}{[M]_0}=1-\left[\frac{f_1}{(f_1)_0}\right]^{\alpha}\left[\frac{1-f_1}{1-(f_1)_0}\right]^{\beta}\left[\frac{(f_1)_0-\delta}{f_1-\delta}\right]^{\gamma} \quad (1)$$

with

$$\alpha=\frac{r_2}{1-r_2}\ \beta=\frac{r_1}{1-r_1}\ \gamma=\frac{1-r_1r_2}{(1-r_1)(1-r_2)}\ \delta=\frac{1-r_2}{2-r_1-r_2}$$

where $1-[M]/[M]_0$ is the conversion, f_1 is the feed composition of NAS at that value of conversion and $(f_1)_0$ is the initial feed composition. The reactivity ratios r_1 and r_2 were obtained for the minimum of the sum of squares of the weighted residuals developed in eq 2:

$$ss(r_1,r_2)=\sum_{i=1}^{n} w_i(y_i-f_i(r_1,r_2))^2 \quad w_i=1/y_i^2 \quad (2)$$

where y_i is the experimental value of conversion at the ith experimental data point and $f_i(r_1, r_2)$ is the theoretical one. This method has the advantage to be not restricted to low conversion values.

Preparation of the Copolymer-Functionalized PLA Nanoparticles

PLA nanoparticles with or without block copolymer as surface modifier were prepared by the dialysis method (diafiltration), initially described by Jeon et al.[33] or nanoprecipitation (solvent diffusion), initially described by Fessi et al.[34] For diafiltration: briefly, 400-mg PLA and 40 or 0 mg of PLA-*b*-P(NAS-*co*-NVP) block copolymer were dissolved in 20 mL of dimethylsulfoxide (DMSO). The solution was introduced into a dialysis tube having a molecular weight cut-off of 6000–8000 g/mol and dialyzed against 4 L of milliQ water for 6 h at room temperature. The water was changed every hour during these 6 h and, subsequently, dialysis was carried out overnight. The day after, water was renewed one last time and after 1 h of dialysis, the nanoparticles were collected from the dialysis tube. The final dispersions had a solid content of typically 1 wt %. No residual DMSO was detected from proton NMR spectra of dissolved particle samples. For nanoprecipitation process, 1.1 g of PLA were dissolved in 50 mL acetone and 0 or 0.11 g of block copolymer in 5-mL acetonitrile. The two organic solutions were mixed and added dropwise through an addition funnel to 35 mL of an aqueous continuous phase under moderate magnetic stirring. The mass transfer of acetone/acetonitrile into the continuous water phase resulted in the formation of PLA nanospheres. After completion, the solvents were removed by evaporation under reduced pressure without heating. No residual acetone was detected from proton NMR spectra of dissolved particle samples, to the sensitivity limits of this method. The final dispersions had a solid content of typically 2.5 wt %.

Nanoparticle Characterization

Nanoparticle size was determined by dynamic light scattering (DLS) at 25 °C, using a Zeta Sizer NanoZS (Malvern instruments, UK). Highly diluted colloidal dispersions in 1-m*M* NaCl solution were used, and each value is at least the average of three measurements. Zeta potentials were measured with Zeta Sizer NanoZS using the same highly diluted samples. The measurements of the electrophoretic mobilities were carried out at 25 °C, and the data were converted to the Zeta potentials using Smoluchowski equation. The values were the average of five measurements. The nanoparticles were observed by scanning electron microscopy (SEM). Few droplets of dispersion (0.1% solid content) were deposited on a Thermanox coverslip and allowed to dry overnight. After mounting on stub and sputtering with gold-palladium, the samples were observed using a FEI Quanta 250 FEG ESEM microscope. UV spectroscopy was used to quantify the available NS groups at the particle surface through the absorbance at 260 nm of the released NHS anion on derivatization with ethanolamine. Typically, to a 2 mL of NP dispersion at 0.024% in NaCl 1 m*M* was added 26 μL of an ethanolamine solution (6.1 mg mL^{-1}). After 15 min, the size and zeta potential of the particles were measured, and the particles were centrifuged at 11,000 rpm for 20 min (in some cases additional centrifugation was necessary). Then, the UV spectrum of the supernatant was recorded with Cary 50 Varian spectrometer and the absorbance (OD) at 260 nm gave access to the NS available groups, through the use of a calibration curve OD = f([NHS]) built up in the same conditions. The surface density (NS groups/nm^2) could be deduced using the specific surface of the particles. The amount of hydrolyzed NS esters could be also evaluated by UV using the same procedure, with the exception that ethanolamine was added in the supernatants after centrifugation. Colloidal stability of the dispersions was evaluated by measuring particle size by DLS in solutions presenting increasing sodium chloride concentrations.

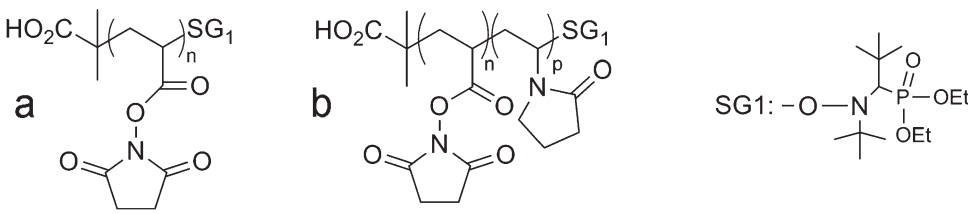

FIGURE 1 Chemical structures of poly(*N*-acryloxysuccinimide) (PNAS) (a) and poly(*N*-acryloxysuccinimide-*co*-*N*-vinylpyrrolidone) (P(NAS-*co*-NVP)) (b) obtained by nitroxide mediated polymerization (NMP) of NAS and NAS/NVP from the MAMA-SG1 alkoxyamine.

RESULTS AND DISCUSSION

NMP of NAS and NAS/NVP from the MAMA-SG1 Alkoxyamine

Before investigating the NMP of NAS/NVP to obtain our desired hydrophilic/functional copolymer, we first focused on the NMP of the NAS alone. Homopolymerization of this monomer by this technique has not been studied up to now, and PNAS is a preactivated polymer of interest in the field of conjugation with biomolecules. NMP was performed in DMF at 110 °C, using the MAMA-SG1 alkoxyamine targeting a M_n of 10,000 g mol^{-1} [Fig. 1(a), for PNAS structure]. The effect of free SG1 nitroxide on the polymerization process was evaluated (0, 2.5, 5, and 7.5 mol % to initiator), because it has been previously reported that for monomers presenting high-propagation rate constant (which is the case for NAS), free SG1 is usually needed to force the equilibrium between the active and dormant species and thus to ensure better control of the polymerization.[35] The introduction of free SG1 in the polymerization medium yielded an improved linearity for $\ln([M]_0/[M])$ versus time (Supporting Information Fig. S1a), indeed suggesting a better polymerization control, even for the lowest SG1 amounts introduced (2.5 mol % to MAMA-SG1). The conditions retained for further studies were 5 mol % SG1 to alkoxyamine.

In these selected conditions, whatever the standards used for GPC calibration, an increase of the PNAS apparent molecular weights was observed along conversion, even if it was less marked as theoretically expected, indicating a relative control of the polymerization (Fig. 2, Supporting Information Fig. S1b for GPC traces). Poly(methyl methacrylate) (PMMA) appeared to be the most appropriate standard for GPC calibration. Finally, the polydispersity index values were quite low, supporting the controlled character of the polymerization.

We then focused on the synthesis by NMP of P(NAS-*co*-NVP) copolymers [Fig. 1(b), for the copolymer structure], in which the NVP units are suitable to improve hydrophilicity for drug delivery applications. The NMP was performed using MAMA-SG1 as initiator, in DMF at 100 °C. Higher polymerization temperatures were reported to induce NVP degradation.[36] Different NAS molar feed for the same targeted total degree of polymerization were investigated to determine the reactivity ratios. The most common procedures for calculating reactivity ratios such as those proposed by Fineman and Ross[37] and by Kelen and Tüdos[38] can only be applied to experimental data at sufficiently low conversion (<5%), because calculation is based on the differential copolymerization equation.[39,40] The extended Kelen–Tüdos method involves a rather more complex calculation, and it can be applied to medium conversion experimental data (~40−50%). With regards to rather high conversion of our copolymerization, we used a non linear least-squares procedure to fit

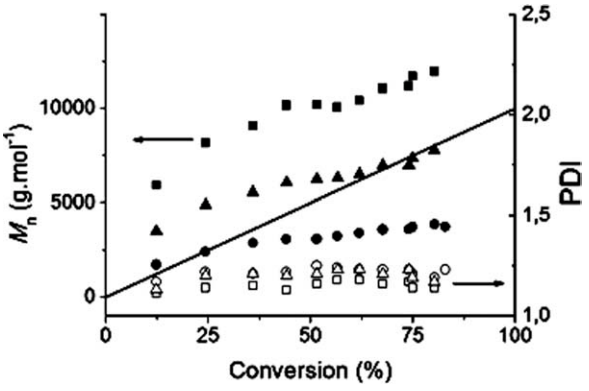

FIGURE 2 Apparent M_n (plain symbols) and PDI (empty symbols) versus conversion for nitroxide mediated polymerization (NMP) of *N*-acryloxysuccinimide (NAS) in DMF at 110 °C, using different polymer standards: PS (squares), PMMA (triangles), and PEG (rounds); thick line is the theoretical curve.

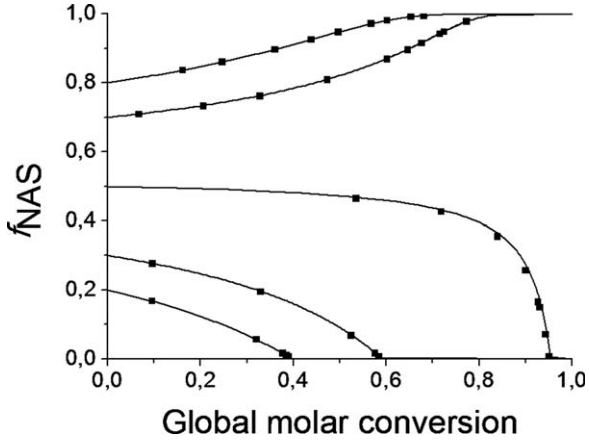

FIGURE 3 *N*-Acryloxysuccinimide (NAS) molar fraction in feed (f_{NAS}) vs global molar conversion for copolymerizations of *N*-acryloxysuccinimide (NAS) and *N*-vinylpyrrolidone (NVP) with 5% of free SG1 to MAMA-SG1 initiator (DMF, 100 °C).

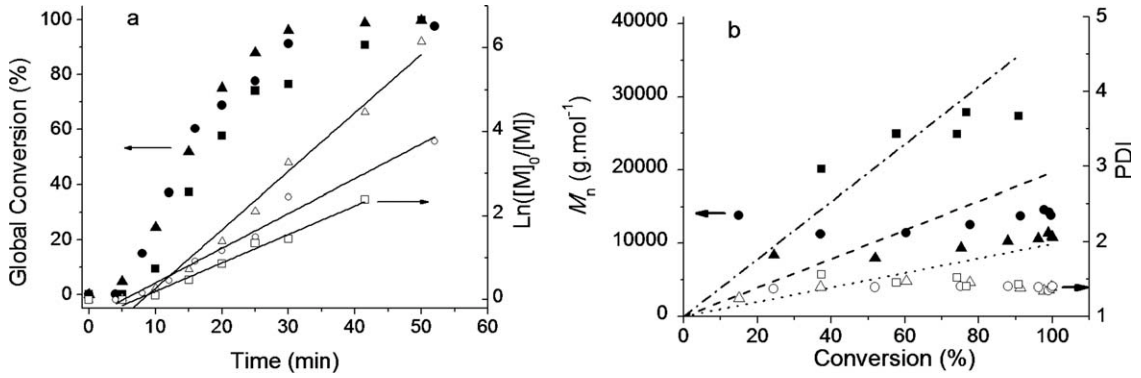

FIGURE 4 Copolymerization of *N*-acryloxysuccinimide (NAS) and *N*-vinylpyrrolidone (NVP) at 100°C, initiated by the MAMA-SG1 alkoxyamine initiator, in presence of free SG1 (5% to initiator): (a) global conversion and $\ln([M]_0/[M])$ vs time; (b) M_n (plain symbols) and PDI (empty symbols) vs conversion for different targeted M_n: 10,000 g mol^{-1} (triangles), 20,000 g mol^{-1} (rounds) and 40,000 g mol^{-1} (squares).

experimental and theoretical values of conversion obtained with the integrated copolymerization equations developed by Lowry and Meyer[32] by minimizing weighted residuals, as previously reported and described in the experimental section. The reactivity ratios were determined to be $r_{NAS} = 0.15$ and $r_{NVP} = 0$ when no free SG1 was added in the polymerization medium, and $r_{NAS} = 0.12$ and $r_{NVP} = 0$ when using 5 mol % SG1 to MAMA-SG1 alkoxyamine (Fig. 3), indicating a very limited impact of the extra free nitroxide on the monomer addition process during the polymerization. The obtained reactivity ratio values were indicative of a strong alternating tendency for the copolymer, similarly as previously reported in an earlier study on copolymerization of the two monomers by conventional radical polymerization ($r_{NAS} = 0.27$ and $r_{NVP} = 0.01$).[27] Interestingly, this induces a homogenous distribution and quite high density of the reactive NS ester functions of the NAS for further biomolecule coupling. Based on the obtained reactivity ratios ($r_{NAS} = 0.12$ and $r_{NVP} = 0$), the azeotropic composition was determined to be at 53% of NAS.

Further studies on the NAS/NVP copolymerization process were then performed using a starting molar fraction in NAS of 0.6. Again, the polymerization was performed in presence of 5 mol % free SG1 to initiator to favor control. Despite lower monomer concentrations and lower temperature used, the copolymerization of NAS with NVP appeared to be much faster than that observed for the NAS homopolymerization [Fig. 4(a)]. The $\ln([M]_0/[M])$ expression relying to the global conversion increased linearly with time for different targeted molecular weights (10,000, 20,000, and 40,000 g mol^{-1}). As shown in Figure 4(b), the molecular weights tended to increase with global conversion and were relatively close to the expected ones (calculated from the relation $M_{n,th} = [NAS]_0 \times M_{NAS} \times conv_{NAS} + [NVP]_0 \times M_{NVP} \times conv_{NVP}]/[MAMA\text{-}SG1]_0$, with $M_{NAS} = 169.1$ g mol^{-1} and $M_{NVP} = 111.1$ g mol^{-1}). In addition, the PDI values tended to decrease with conversion and did not exceed 1.4, indicating a relative control of the polymerization.

NMP of NAS/NVP from the PLA-SG1 Macro-Alkoxyamine

We then focused on the synthesis of PLA-*b*-P(NAS-*b*-NVP) block copolymers, to use them as surface modifiers in the fabrication process of PLA nanoparticles. To obtain them, our approach was based on the use of a SG1 functionalized PLA macro-alkoxyamine as initiator for the NMP of NAS/NVP (Scheme 1). This macro-alkoxyamine was obtained as previously described in our group by performing a 1,2-

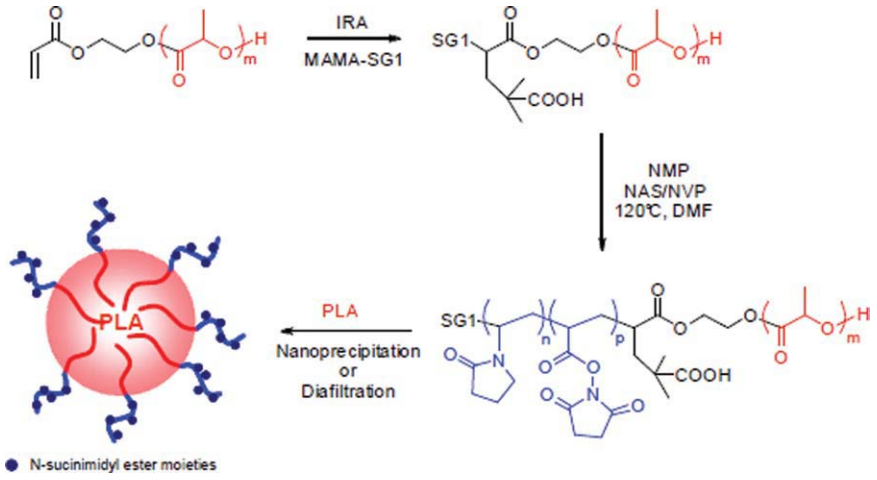

SCHEME 1 Strategy of synthesis for PLA-*b*-P(NAS-*co*-NVP) copolymer, using a PLA-SG1 macro-alkoxyamine as initiator for NMP of NAS/NVP, and further nanoparticle preparation.

TABLE 1 Characteristics of the Different PLA-*b*-P(NAS-*co*-NVP) Block Copolymers Synthesized Through NMP of NAS/NVP from PLA-SG1 Macro-Alkoxyamine (NAS Molar Composition Feed of 0.6)

Copolymer Code	M_n PLA Block[a] (g mol^{-1})	M_n P(NAS-*co*-NVP)[b] Block (g mol^{-1})	PDI
BC1	19,000	17,000	1.64
BC2	19,000	12,000	1.34
BC3	10,500	11,000	1.62

[a] Determined by GPC from universal calibration.[15]
[b] Determined by ^{1}H NMR integration.

intermolecular radical addition (IRA) of the MAMA-SG1 alkoxyamine onto acrylate end-capped PLA previously prepared by ROP.[15] The NMP of NAS/NVP from this macroinitiator was performed in DMF at 120 °C. This polymerization temperature, higher than that used for the NMP previously run from the MAMA-SG1, was chosen to favor the initiation efficiency of NMP, because we showed in earlier studies that the activation energy for dissociation of PLA-SG1 macroalkoxyamine is higher than that of MAMA-SG1.[15] In addition, this higher temperature was found not to be prejudicial regarding NVP integrity due to the short polymerization times. The found NAS and NVP reactivity ratios were 0.17 and 0.02, respectively, very close to those previously obtained, as expected, confirming the alternating tendency for the P(NAS-*co*-NVP) block. In Table 1 are compiled the different molar masses of block copolymers prepared (with a molar feed in NAS of 0.6). The molecular weight of the P(NAS-*co*-NVP) block was obtained from ^{1}H NMR integration (Fig. 5) on the spectrum of the purified block copolymer after precipitation in diethyl ether/methanol, based on the known molar mass of the PLA block. In Figure 6 are represented the ^{1}H NMR spectra of the crude mixtures in the course of NMP of NAS and NVP from the PLA-SG1. Besides the progressive decreasing of the monomer proton signals concomitant with increasing ones from the forming polymer, it is to point out (in the range of 1–1.5 ppm) the shift of the ^{t}Bu protons of the SG1 moiety along the polymerization process, as a result of its environment change (the SG1 initially linked to the PLA α-end group becomes adjacent to the NAS/NVP, Scheme 1). This supports a quite good initiation efficiency of the NMP from PLA-SG1. The polydispersity index obtained by SEC was quite acceptable (Table 1).

Functionalized PLA Nanoparticles

The block copolymer was then used with PLA homopolymer (M_n = 30,000 g mol^{-1}) in the nanoparticle formation process, to achieve both hydrophilic and densely NS ester-functionalized nanoparticles at their surface (Scheme 1, last step). Nanoprecipitation and diafiltration processes were used to reach size ranges of about 150 and 500 nm, respectively. For nanoprecipitation, both polymers were first dissolved in acetone/acetonitrile (the copolymer was indeed insoluble in pure acetone, which is the solvent classically used in the PLA nanoprecipitation process). The nanoparticles formed instantaneously on addition of this polymer organic phase into water, as a result of rapid diffusion of the acetone/acetonitrile solvents in the water phase. The organic solvents were then removed under reduced pressure. As for diafiltration, PLA and the copolymer were dissolved in DMSO, and the solution was dialyzed against water for several hours, with periodic changes of water bath. The nanoparticles formed slowly as a result of progressive replacement of DMSO by water in the dialysis bag. As both methods are known to be surfactant free, reference-naked PLA particles were also prepared using the same procedure for both

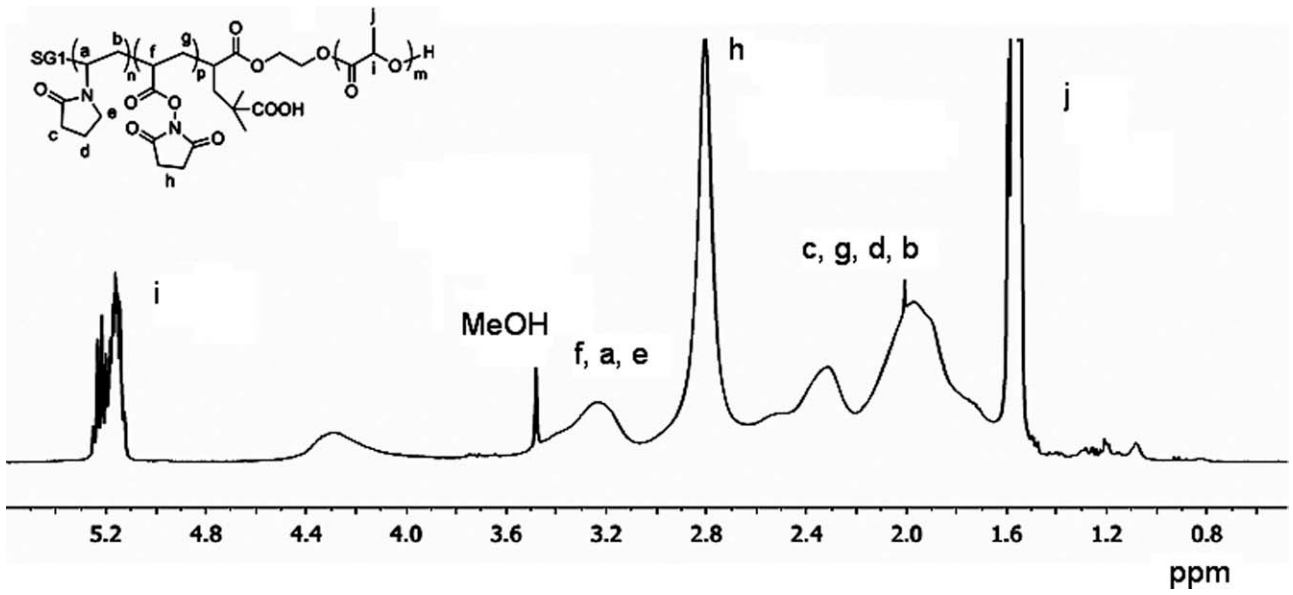

FIGURE 5 ^{1}H NMR spectrum ($CDCl_3$) of the PLA-*b*-P(NAS-*co*-NVP) block copolymer after precipitation in 1/1 diethylether/methanol mixture.

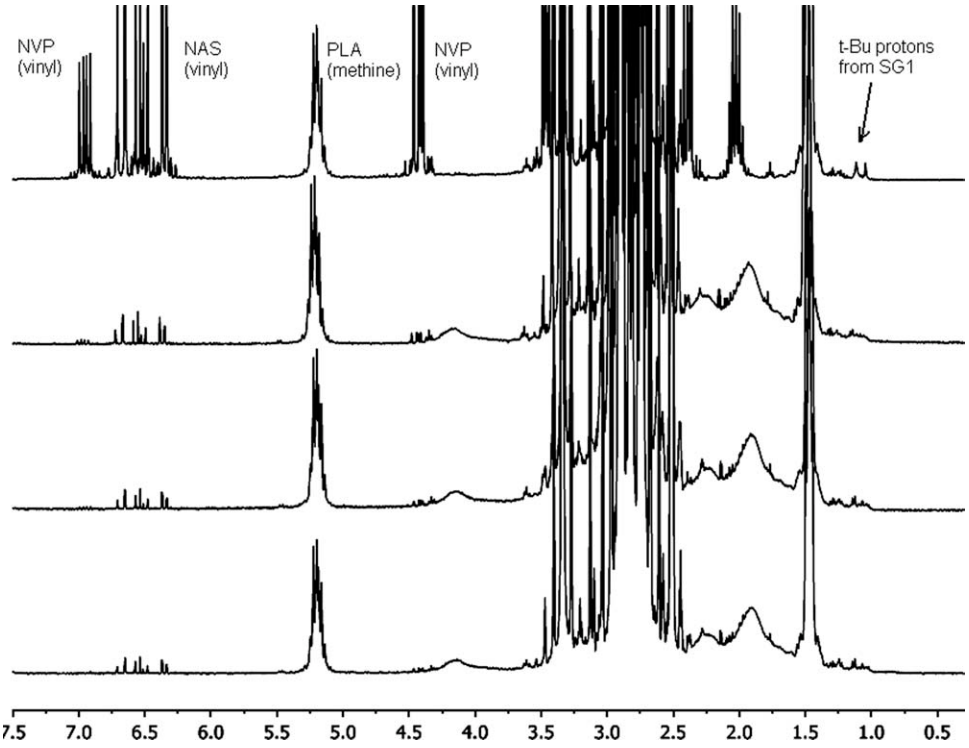

FIGURE 6 ^{1}H NMR spectra of crude polymerization mixtures along NAS/NVP conversion for the NMP of NAS/NVP from PLA-SG1 macro-alkoxyamine (15, 30, 45, and 60 min polymerization times, from top to bottom).

processes, but in the absence of block copolymer. The characteristics of the obtained nanoparticles are presented in Table 2. All the nanoparticles presented a rather homogeneous distribution in size, as shown by the polydispersity index values given by DLS, close to 0.1 in most cases, as well as no aggregation (Supporting Information Fig. S2 for the size distribution profiles). These results were confirmed by SEM analysis of the nanoparticles (Fig. 7). Interestingly, naked PLA particles [NP0, Fig. 7(b)] tended to more collapse than functionalized nanoparticles [NP1, Fig. 7(a)] under exposition to the electron beam heating, strongly suggesting the contribution of the NAS/NVP-based copolymer at the particle surface to prevent PLA filmification.

The particles prepared in the presence of copolymer were slightly bigger than the naked particles for the nanoprecipitation process, whereas no significant differences were observed between naked and copolymer-functionalized particles obtained by diafiltration (Table 2). Nevertheless, for both processes, the zeta potential significantly changed, and was much less negative for nanoparticles prepared in the presence of copolymer than for the naked ones, indicating the contribution of the hydrophilic/functional neutral copolymer at the particle surface. The still negative zeta potential for the copolymer-functionalized nanoparticles was ascribed to the partial hydrolysis of the NS esters in water, as previously described[18] and pointed out later.

NP1 and DIA1 copolymer-functionalized nanoparticles were compared with NP0 and DIA0 naked nanoparticles as reference, respectively, by means of colloidal stability in the presence of salt. A marked difference in colloidal stability was observed between both kinds of nanoparticles, as evidenced by size measurements as a function of sodium chloride concentration. DIA0 flocculated at less than 0.5*M* salt concentration, whereas DIA1 remained stable until at least 1.5*M*. Similar results were obtained for the bigger NP1 and NP0 particles. Such higher colloidal stability for NP1 and DIA1 can clearly be attributed to the influence of the copolymer at the interface, responsible for a steric contribution to the stabilization of the particles, which corroborates the zeta potential measurements. To further evidence the presence and availability of the activated esters at the particle surface for further coupling of biomolecules, ethanolamine as a model reactive compound was added in excess (compared with

TABLE 2 Characteristics of the Functionalized PLA Nanoparticles (10 wt % Copolymer with Respect to Homo-PLA) and Naked PLA Particles

NP Code	Copolymer	Process	Average Diameter[a] (nm)	PI[b]	Zeta Potential ξ (mV)
NP0	–	Nanoprec.	126	0.099	−69
NP1	BC1	Nanoprec.	156	0.095	−60
NP2	BC2	Nanoprec.	180	0.160	−45
NP3	BC3	Nanoprec.	204	0.130	−45
DIA0	–	Diafiltration	461	0.098	−75
DIA1	BC1	Diafiltration	435	0.195	−40
DIA2	BC2	Diafiltration	451	0.086	−55
DIA3	BC3	Diafiltration	452	0.088	−35

[a] Average hydrodynamic particle size.
[b] Polydispersity index given by DLS.

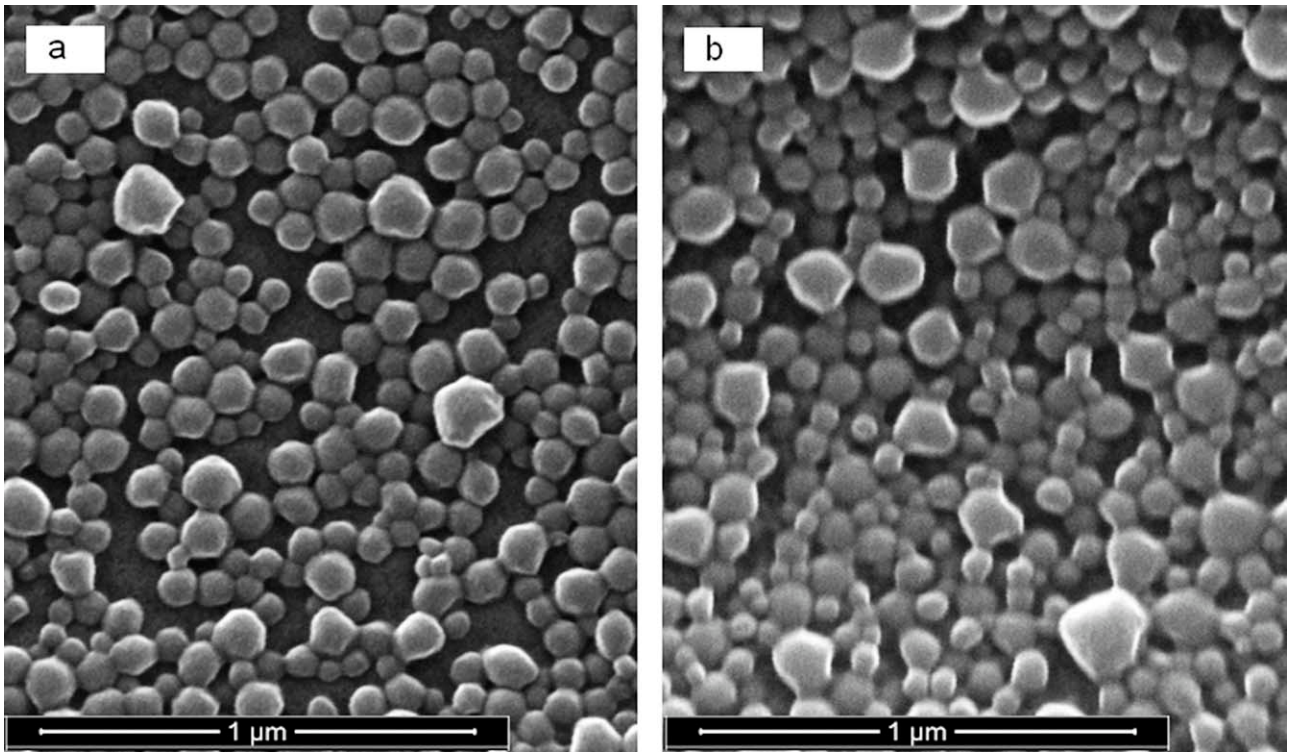

FIGURE 7 Scanning electron microscopy images of the NP1 (a) and NP0 (b) nanoparticles.

activated NS ester functions) in both naked and copolymer-functionalized PLA nanoparticle dispersions (in NaCl 0.001*M*). After ethanolamine adding, the diameter of the reference naked NP0 particles remained constant (127 nm) and the zeta potential became even more negative (−80 mV), as a result of the fully deprotonation of carboxylic acid moities at the particle surface (Table 3). In contrast, the diameter of the copolymer-functionalized particles (NP1) significantly increased (from ∼20 nm), and the zeta potential increased to −40 mV, compared to −60 mV before addition. This was due to the reaction of amine of ethanolamine with the NS-activated esters of the surface of the particle, which renders the particle corona highly hydrophilic and, as a result, favor its expansion toward aqueous medium. Consequently, the zeta potential was logically increased (reduced in absolute value) due to the shielding by this newly formed neutral corona based on *N*-vinylpyrrolidone and hydroxyethyl pendant groups of the copolymer. The still negative value was explained by the carboxylates arising from the NAS prehydrolysis and competitive hydrolysis by water, due to the drastically increased pH of the continuous phase of the dispersion.

The reaction of ethanolamine with the activated esters was finally confirmed by UV measurements. Indeed, the UV spectrum of the supernatant after ethanolamine adding to the NP1 dispersion and centrifugation, clearly evidenced the presence of the released *N*-hydroxysuccinimide (NHS) anion, with its typical maximum absorption wavelength at 260 nm (Supporting Information Fig. S3), as a result of ethanolamine nucleophilic attack on the activated NS ester. The naked PLA particles after ethanolamine adding did not exhibit any UV absorption, as expected (Supporting Information Fig. S3). Based on a calibration curve built up in the same conditions (OD as a function of NHS concentration in ethanolamine basic conditions), the surface density of the NS ester groups available at the particle surface for coupling could be determined to be about 4 μmol m^{-2}, that is, 2.4 groups nm^{-2}, which was quite high. The particles remained stable under storage at 4 °C in terms of size. Indeed, after 3 months, the

TABLE 3 Effect of Ethanolamine Addition in the NP Dispersion on the Size and Zeta Potential

	Before Adding Ethanolamine			After Adding Ethanolamine		
NP Code	Average Diameter (nm)	PI	ξ (mV)	Average Diameter (nm)	PI	ξ (mV)
NP0	126	0.099	−69	127	0.105	−80
NP1	156	0.095	−60	176	0.080	−40

particle mean diameter and polydispersity index given by dynamic light scattering remained quasi the same. However, pronounced hydrolysis of the activated esters was shown to proceed with time (as also pointed out earlier[18]). The amount of hydrolyzed esters could be obtained by measuring the OD by adding the ethanolamine in the supernatant of the particle dispersions after centrifugation. After 3 months, the fraction of hydrolyzed esters on the total available was determined to be more than 75%. This was confirmed by the poor colloidal stability of the dispersion with a flocculation observed at less than 0.5*M* NaCl, showing that the esters were hydrolyzed to carboxyl ionic groups thus reducing the steric contribution to stabilization. This underlines that the reactive groups of these promising novel functionalized PLA nanoparticles should be used within a limited time after preparation, if not freeze-dried.

CONCLUSIONS

In this work, MAMA-SG1 alkoxyamine-initiated NMP was successfully applied to synthesis of well-defined PNAS and P(NAS-*co*-NVP) polymers. The homopolymerization of NAS was controlled in the presence of SG1. A strong alternating tendency was observed for the copolymerization of NAS with NVP and the obtained copolymers exhibited acceptable polydispersities and adjustable molecular weights, consistent with a controlled process. The NMP of NAS/NVP was then initiated with a PLA-SG1 macro-alkoxyamine previously prepared, leading to PLA-*b*-P(NAS-*co*-NVP) block copolymer. The latter was involved as a particle surface modifier in the PLA nanopreciptation and diafiltration processes, to achieve nanoparticles of targeted size with a hydrophilic and highly functionalized interface. The presence of the NS reactive groups was clearly evidenced by zeta potential, colloidal stability measurements and UV-based determination of the releasing NHS anion upon ethanolamine derivatization. We are currently focusing on the freeze-drying process of these particles to limit NS ester hydrolysis and investigating the coupling on these novel particles of ligands such as mannosamine or immunostimulating molecules for further vaccine delivery applications.

The authors are grateful to Arkema, Université de Provence and CNRS for financial support and Marilyne Malbouyres (IBCP) and Béatrice Burdin from the Centre Technologique des Microstructures (Lyon, France) for SEM experiments. Part of this work has been funded through two grants from European Union (Europrise and Cuthivac) to E. Luciani and B. Verrier.

REFERENCES AND NOTES

1 Jalil, R.; Nixon, J. R. J Microencapsul 1990, 7, 297–325.

2 Mundargi, R. C.; Babu, V. R.; Rangaswamy, V.; Patel, P.; Aminabhavi, T. M. J Control Release 2008, 125, 193–209.

3 (a) Zhuang, X.; Xiao, C.; Oyaizu, K.; Chikushi, N.; Chen, X.; Nishide, H. J Polym Sci Part A: Polym Chem 2010, 48, 5404–5410; (b) Sun, L.; Shen, L.-J.; Zhu, M.-Q.; Dong, C.-M.; Wei, Y. 2010, 48, 4583–4593; (c) Nottelet, B.; Di Tommaso, C.; Mondon, K.; Gurny, R.; Möller, M. J Polym Sci Part A: Polym Chem 2010, 48, 3244–3254; (d) Jubeli, E.; Moine, L.; Barratt, G. J Polym Sci Part A: Polym Chem 2010, 48, 3178–3187.

4 Avgoustakis, K. Curr Drug Deliv 2004, 1, 321–333.

5 Rieger, J.; Freichels, H.; Imberty, A.; Putaux, J. L.; Delair, T., Jerome, C.; Auzely-Velty, R. Biomacromolecules 2009, 10, 651–657.

6 Nagasaki, Y.; Yasugi, K.; Yamamoto, Y.; Harada, A.; Kataoka, K. Biomacromolecules 2001, 2, 1067–1070.

7 Yamamoto, Y.; Nagasaki, Y.; Kato, Y.; Sugiyama, Y.; Kataoka, K. J Control Release 2001, 77, 27–38.

8 Betancourt, T.; Byrne, J. D.; Sunaryo, N.; Crowder, S. W.; Kadapakkam, M.; Patel, S.; Casciato, S.; Brannon-Peppas, L. J Biomed Mater Res A 2009, 91, 263–276.

9 Theato, P. J Polym Sci Part A: Polym Chem 2008, 46, 6677–6687.

10 Knop, K.; Hoogenboom, R.; Fischer, D.; Schubert, U. S. Angew Chem Int Ed 2010, 49, 6288–6308.

11 Dove, A. P. Chem Commun 2008, 6446–6470.

12 (a) Sha, K.; Li, D.; Wang, S.; Qin, L.; Wang, J. Polym Bull 2005, 55, 349–355; (b) de Geus, M.; Peeters, J.; Wolffs, M.; Hermans, T.; Palmans, A. R. A.; Koning, C. E.; Heise, A. Macromolecules 2005, 38, 4220–4225; (c) Likhitsup, A.; Parthiban, A.; Chai, C. L. L. J Polym Sci Part A: Polym Chem 2008, 46, 102–116; (d) Meyer, U.; Palmans, A. R. A.; Loontjens, T.; Heise, A. Macromolecules 2002, 35, 2873–2875; (e) Smith, A. P.; Fraser, C. L. Macromolecules 2003, 36, 2654–2660.

13 (a) You, Y. Z.; Hong, C. Y.; Wang, W. P.; Lu, W. Q.; Pan, C. Y. Macromolecules, 2004, 37, 9761–9767; (b) Li, J. B.; Ren, J.; Cao, Y.; Yuan, W. Z. Polymer 2010, 51, 1301–1310; (c) Ozturk, T.; Goktas, M.; Hazer, B. J App Polym Sci 2010, 117, 1638–1645.

14 (a) van As, B. A. C.; Thomassen, P.; Kalra, B.; Gross, R. A.; Meijer, E. W.; Palmans, A. R. A.; Heise, A. Macromolecules 2004, 37, 8973–8977; (b) Pratt, R. C.; Lohmeijer, B. G. G.; Long, D. A.; Pontus Lundberg, P. N.; Dove, A. P.; Li, H.; Wade, C. G.; Waymouth, R. M.; Hedrick, J. L. Macromolecules 2006, 39, 7863–7871; (c) Nederberg, F.; Lohmeijer, B.; G. G.; Leibfarth, F.; Pratt, R. C.; Choi, J.; Dove, A. P.; Waymouth, R. M.; Hedrick, J. L. Biomacromolecules 2007, 8, 153–160.

15 Clément, B.; Trimaille, T.; Alluin, O.; Gigmes, D.; Mabrouk, K.; Féron, F.; Decherchi, P.; Marqueste, T.; Bertin, D. Biomacromolecules 2009, 10, 1436–1445.

16 Zhang, J.; Jiang, X.; Zhang, Y.; Li, Y.; Liu, S. Macromolecules 2007, 40, 9125–9132.

17 Rowe, M. D.; Thamm, D. H.; Kraft, S. L.; Boyes, S. G. Biomacromolecules 2009, 10, 983–993.

18 Li, Y.; Lokitz, B. S.; McCormick, C. L. Macromolecules 2006, 39, 81–89.

19 Relogio, P.; Charreyre, M.-T.; Farinha, J. P. S.; Martinho, J. M. G.; Pichot, C. Polymer 2004, 45, 8639–8649.

20 Pascual, S.; Monteiro, M. J. Eur Polym J 2009, 45, 2513–2519.

21 Kakwere, H.; Perrier, S. J Am Chem Soc 2009, 131, 1889–1895.

22 Favier, A.; D'Agosto, F.; Charreyre, M.-T.; Pichot, C. Polymer 2004, 45, 7821–7830.

23 Li, Y.; Akiba, I.; Harrisson, S.; Wooley, K. L. Adv Funct Mater 2008, 18, 551–559.

24 De Lambert, B.; Chaix, C.; Charreyre, M.-T.; Martin, T.; Aigoui, A.; Perrin-Rubens, A.; Pichot, C.; Mandrand, B. Anal Biochem 2008, 373, 229–238.

25 Yu, X.; Tang, X. Z.; Pan, C. Y. Polymer 2005, 46, 11149–11156.

26 Fukukawa, K.; Rossin, R.; Hagooly, A.; Pressly, E. D.; Hunt, J. N.; Messmore, B. W.; Wooley, K. L.; Welch, M. J.; Hawker, C. J. Biomacromolecules 2008, 9, 1329–1339.

27 Erout, M.-N.; Elaissari, A.; Pichot, C.; Llauro, M.-F. Polymer 1996, 37, 1157–1165.

28 Yamanaka, H.; Yoshizako, K.; Akiyama, Y.; Sota, H.; Hasegawa, Y.; Shinohara, Y.; Kikuchi, A.; Okano, T. Anal Chem 2003, 75, 1658–1663.

29 Arehart, S. V.; Matyjaszewski, K. Macromolecules 1999, 32, 2221–2231.

30 Van Herk, A. J Chem Educ 1995, 72, 138–140.

31 Van Herk, A.; Dröge, T. Macromol Theor Simul 1997, 6, 1263–1276.

32 Meyer, V. E.; Lowry, G. G. J Polym Sci Part A: Polym Chem 1965, 3, 2843–2851.

33 Jeon, H. J.; Jeong, Y. I.; Jang, M. K.; Park, Y. H.; Nah, J. W. Int J Pharm 2000, 207, 99–108.

34 Fessi, H.; Devissaguet, J.-P.; Puisieux, F.; Thies, C. U.S. Patent 5,118,528, European Patent EP0275796B2, December 31, 1986.

35 (a) Gigmes, D.; Bertin, D.; Lefay, C.; Guillaneuf, Y. Macromol Theor Simul 2009, 18, 402–419; (b) Chauvin, F.; Dufils, P.-E.; Gigmes, D.; Guillaneuf, Y.; Marque, S. R. A.; Tordo, P.; Bertin, D. Macromolecules 2006, 39, 5238–5250.

36 Bilalis, P.; Pitsikalis, M.; Hadjichristidis, N. J Polym Sci Part A: Polym Chem 2005, 44, 659–665.

37 Fineman, M.; Ross, S. D. J Polym Sci 1950, 5, 259–265.

38 Kelen, T.; Tüdös, F. J Macromol Sci Chem A 1975, 9, 1–27.

39 Mayo, F. R.; Lewis, F. M. J Am Chem Soc 1944, 66, 1594–1601.

40 Alfrey, T.; Goldfinger, G. J Chem Phys 1944, 12, 205–209.